

Supplementary Materials:

The stability of magnetic chitosan beads for adsorption of Cu²⁺

1 Kinetic, isothermal and thermodynamic studies

1.1 Kinetic studies

To explore the mechanism of sorption and potential rate-controlling step, the experimental data were analyzed according to the linearized form of pseudo-first-order and the pseudo-second-order kinetics models. The pseudo-first-order equation could be expressed as Eq. (S1).

$$\log(Q_e - Q_t) = \log Q_e - \frac{k_1}{2.303} t \quad (\text{S1})$$

Where Q_e (mg g⁻¹) is the equilibrium capacity and Q_t (mg g⁻¹) is the adsorption capacity at time t (min); t (min) is the sorption time; k_1 (min⁻¹) is the rate constants of pseudo-first order. The values of $\log(Q_e - Q_t)$ were calculated from the kinetic data

The pseudo-second-order equation could be expressed as Eq.(S2).

$$\frac{t}{Q_t} = \frac{1}{k_2 Q_e^2} + \frac{t}{Q_e} \quad (\text{S2})$$

Where k_2 (g mg⁻¹ min⁻¹) are the rate constants of pseudo-second order adsorption, respectively. The kinetic adsorption data were fitted to Eqs. (S1) and (S2), and the calculated results were given in **Table S1**.

Table S1

The pseudo-first order and pseudo-second order adsorption constants, calculated and experimental Q_e value for different initial Cu²⁺ concentrations.

Parameter	Q_e (mg g ⁻¹)	Pseudo-first order			Pseudo-second order		
		K_1 (min ⁻¹)	$Q_{e,cal}$ (mg g ⁻¹)	R^2	K_2 (mg g ⁻¹ min)	$Q_{e,cal}$ (mg g ⁻¹)	R^2
Initial Cu ²⁺ concentration (mg/g) $t=150$ min, pH 4, 30 °C							
100	64.5	2.7682×10^{-2}	25.06	0.9532	4.9064×10^{-3}	65.79	0.9999
210	90	3.9381×10^{-2}	64.53	0.93502	1.7809×10^{-3}	92.59	0.9996
513	148	4.1454×10^{-2}	172.98	0.9558	0.4708×10^{-3}	156.25	0.9998
750	163	4.6060×10^{-2}	179.06	0.9549	0.6096×10^{-3}	169.49	0.9993

1.2 Isothermal studies

The adsorption equilibrium data was fitted to Langmuir and Freundlich isotherm models.

The equations were expressed as follows:

Langmuir equation:

$$\frac{C_e}{Q_e} = \frac{C_e}{Q_m} + \frac{1}{Q_m K_L} \quad (S3)$$

Where K_L is the Langmuir constant ($L\ mg^{-1}$), Q_m is the maximum sorption capacity ($mg\ g^{-1}$), C_e is the equilibrium Cu^{2+} concentration ($mg\ L^{-1}$) in aqueous solution.

Freundlich equation:

$$\log Q_e = b_F \log C_e + \log K_F \quad (S4)$$

Where K_F ($mg\ g^{-1}$) and b_F are the empirical constants, they indicate the relative sorption capacity and sorption intensity, respectively.

Table S2

Adsorption equilibrium isotherm

Freundlich			Langmuir		
K_F ($mg\ g^{-1}$)	b_F	R^2	Q_m ($mg\ g^{-1}$)	K_L ($L\ g^{-1}$)	R^2
15.9038	0.36698	0.09050	167.22	0.0271	0.9935

1.3 Thermodynamic studies

In order to obtain the thermodynamics involved in the adsorption of Cu^{2+} by MCBs, the experiments were performed at temperatures of 293, 303, 313 K, and the initial Cu^{2+} concentration of 20-750 $mg\ L^{-1}$.

Thermodynamic parameters can be calculated from the variation of the thermodynamic equilibrium constant K_0 with the change in temperature. For adsorption reactions, K_0 is defined as follows:

$$K_0 = \frac{a_s}{a_e} = \frac{v_s C_s}{v_e C_e} \quad (S5)$$

Where a_s is the activity of adsorbed Cu^{2+} , a_e is the activity of Cu^{2+} in solution at equilibrium, v_s and v_e are the activity coefficients of adsorbed Cu^{2+} and Cu^{2+} in solution at equilibrium, respectively, C_s is the amount of Cu^{2+} absorbed by MCBs ($mmol\ g^{-1}$), and C_e is the concentration

of Cu^{2+} in solution at equilibrium (mmol mL^{-1}). Values of K_0 can be obtained by plotting $\ln(C_s/C_e)$ versus C_s and extrapolating to $C_s=0$ (**Fig. 5(C)**). The straight line obtained is fitted to the points based on a least-squares analysis. Its intercept with the vertical axis gives the values of K_0 ^{S1-S3}.

According to the isothermal equation (Eq. (S6)) and the Van't Hoff equation (Eq. (S7)) as follows:

$$\Delta G^0 = -RT \ln K_0 \quad (\text{S6})$$

$$\ln K_0 = \frac{\Delta H^0}{RT} + \frac{\Delta S^0}{R} \quad (\text{S7})$$

Where R is the gas constant ($8.314 \text{ J mol}^{-1} \text{ K}^{-1}$), and T is the absolute temperature in Kelvin. ΔH^0 is standard enthalpy change (kJ mol^{-1}) and ΔS^0 is standard entropy change ($\text{J mol}^{-1} \text{ K}^{-1}$).

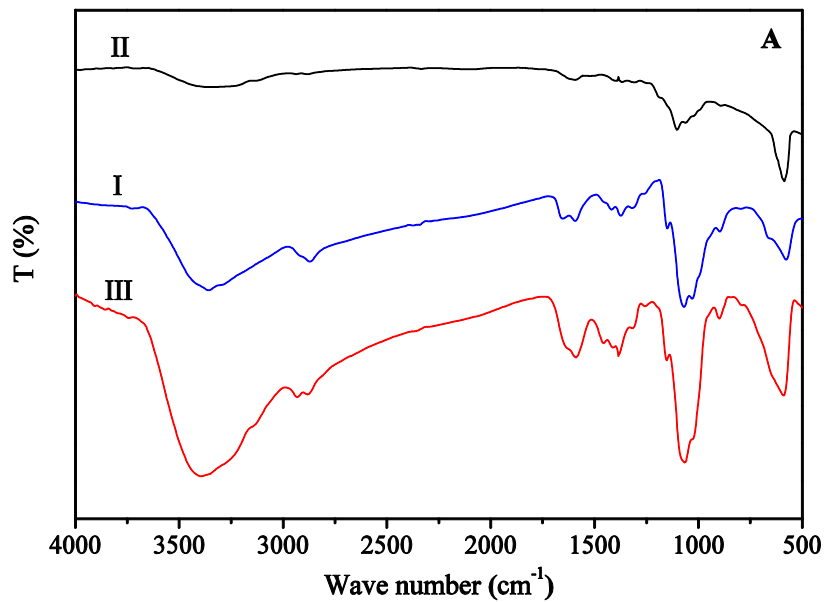
Table S3

Thermodynamic parameters for adsorption of Cu^{2+} on MCBs

T (K)	K_0	ΔG^0 (kJ mol^{-1})	ΔH^0 (kJ mol^{-1})	ΔS^0 $\text{J mol}^{-1} \text{ K}^{-1}$
293	2.603	-5.620		
303	2.513	-6.331	-4.579	76.027
313	2.307	-6.774		

2 Characterization of MCBs in various conditions

2.1 FTIR and XRD analysis of MCBs in the regeneration process



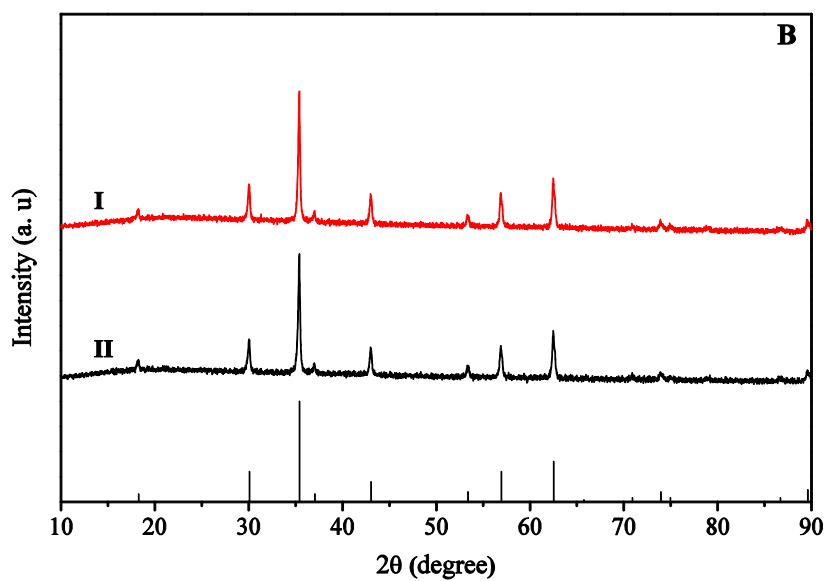
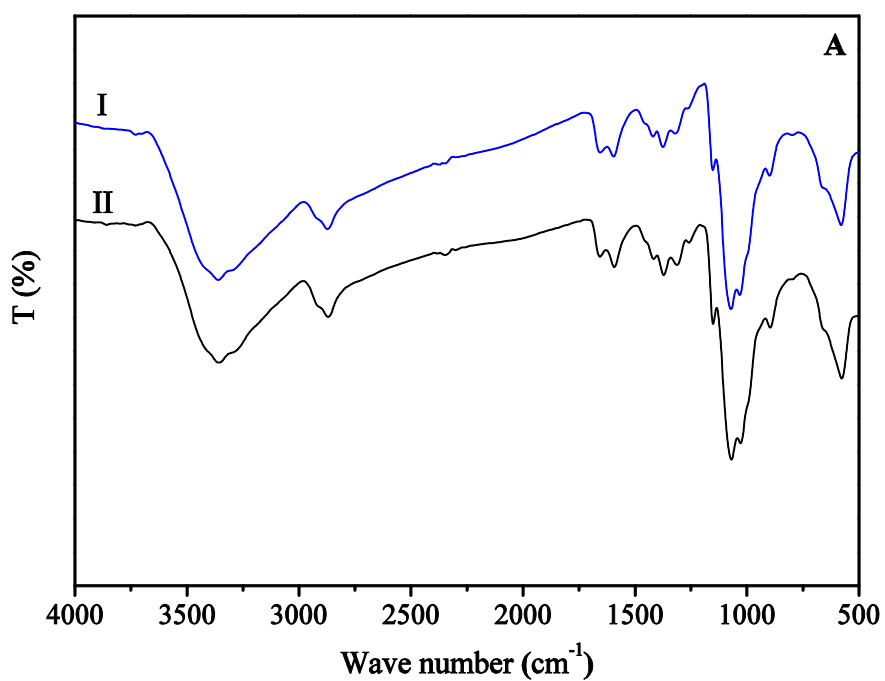


Fig. S1. (A) FTIR spectra of original MCBs(I), Cu²⁺ loaded MCBs(II), and MCBs after desorption (III). (B) XRD patterns of MCBs adsorbed Cu²⁺(I) and regenerated(II). (Literature values for the peak positions and intensities for bulk magnetite samples are indicated by the vertical bars).

2.2 FTIR and XRD analysis of MCBs stored for ten months



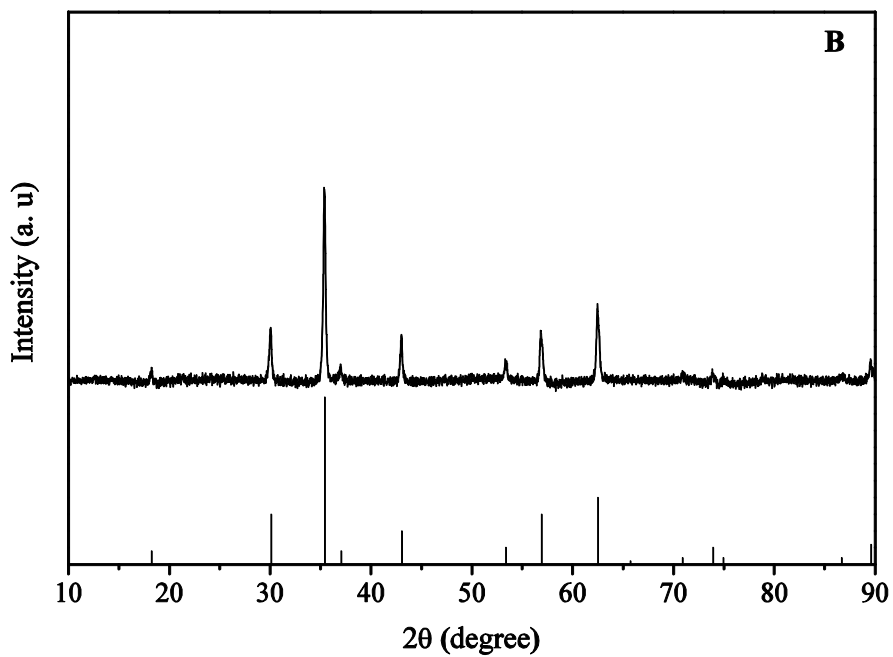
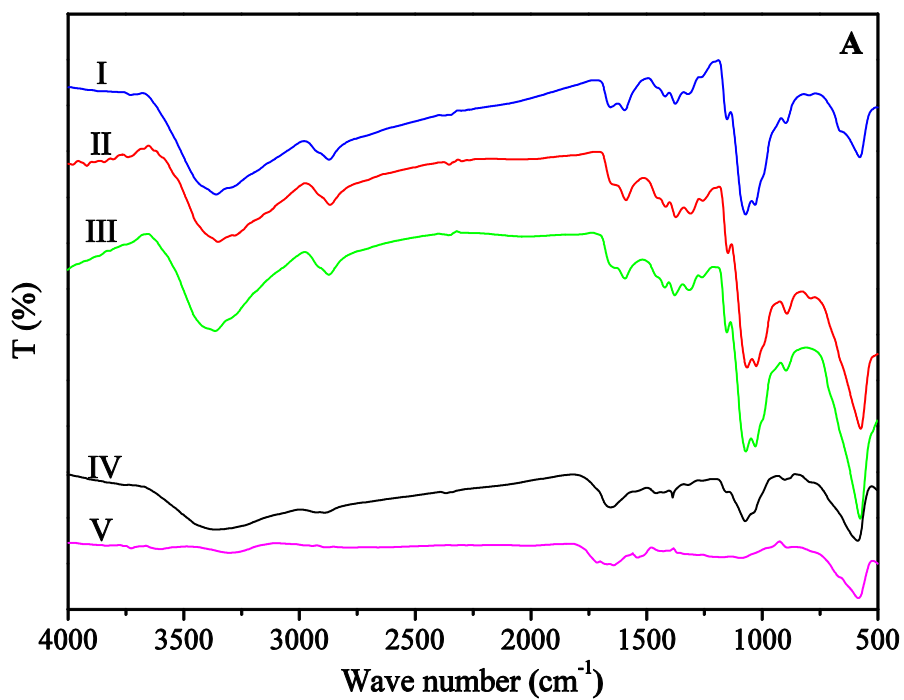


Fig. S2 (A) FTIR spectra of original MCBs(I) and MCBs stored for ten months(II). **(B)** XRD of MCBs stored for ten months. (Literature values for the peak positions and intensities for bulk magnetite samples are indicated by the vertical bars)

2.3 FTIR and XRD analysis of MCBs heated under atmosphere and vacuum



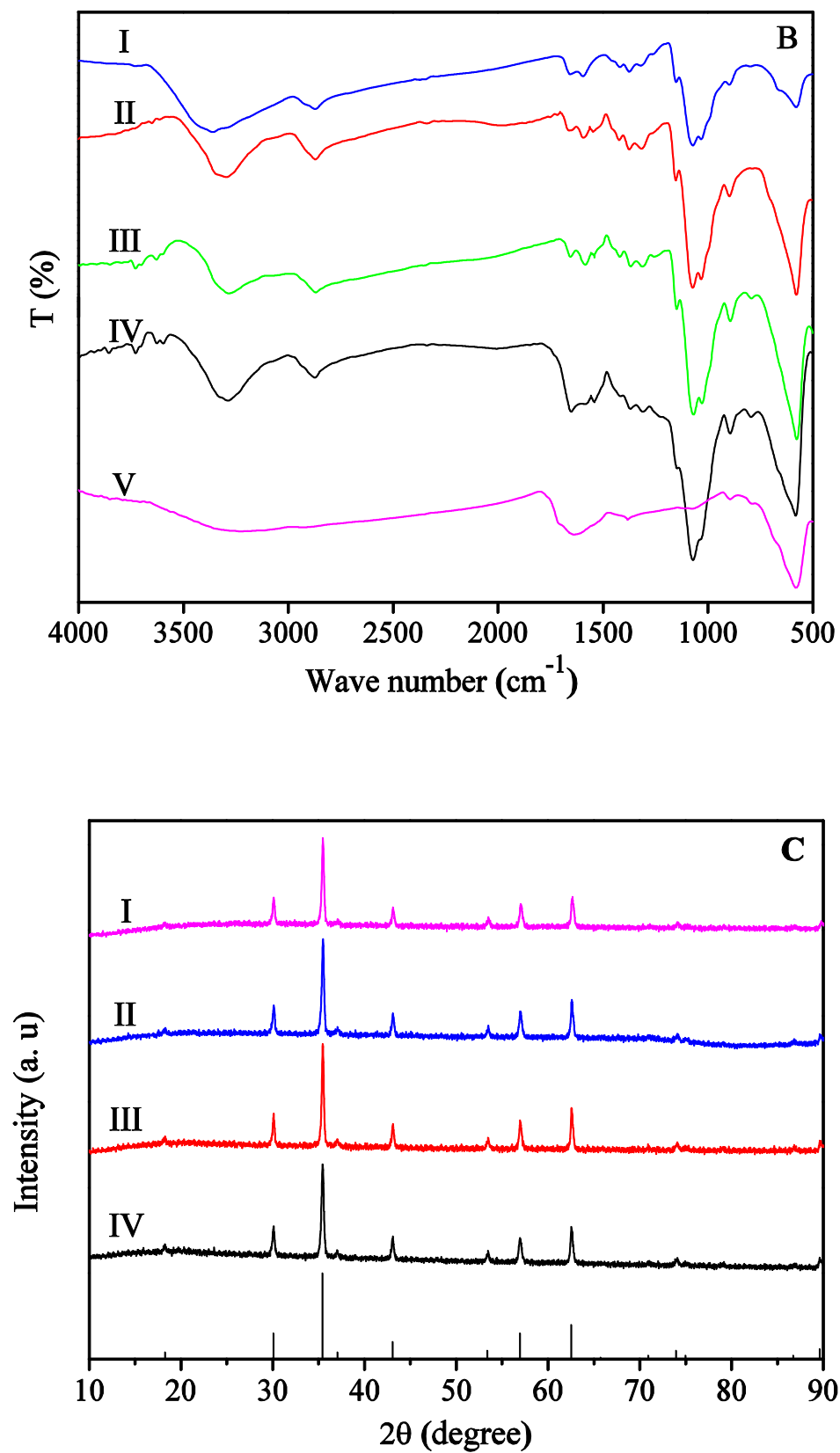


Fig. S3. FTIR spectra of MCBs heated under atmosphere(A) and vacuum(B) with different temperature for 30 h: original MCBs (I), 50 °C (II), 100 °C (III), 150 °C(IV), 200 °C (V). (C) XRD of MCBs heated in air blast oven (150 °C (I) and 200 °C (II)) and vacuum oven (150 °C (III) and 200 °C (IV)). (Literature values for the peak

positions and intensities for bulk magnetite samples are indicated by the vertical bars)

2.4 FTIR and XRD analysis of MCBs stored at different magnetic fields

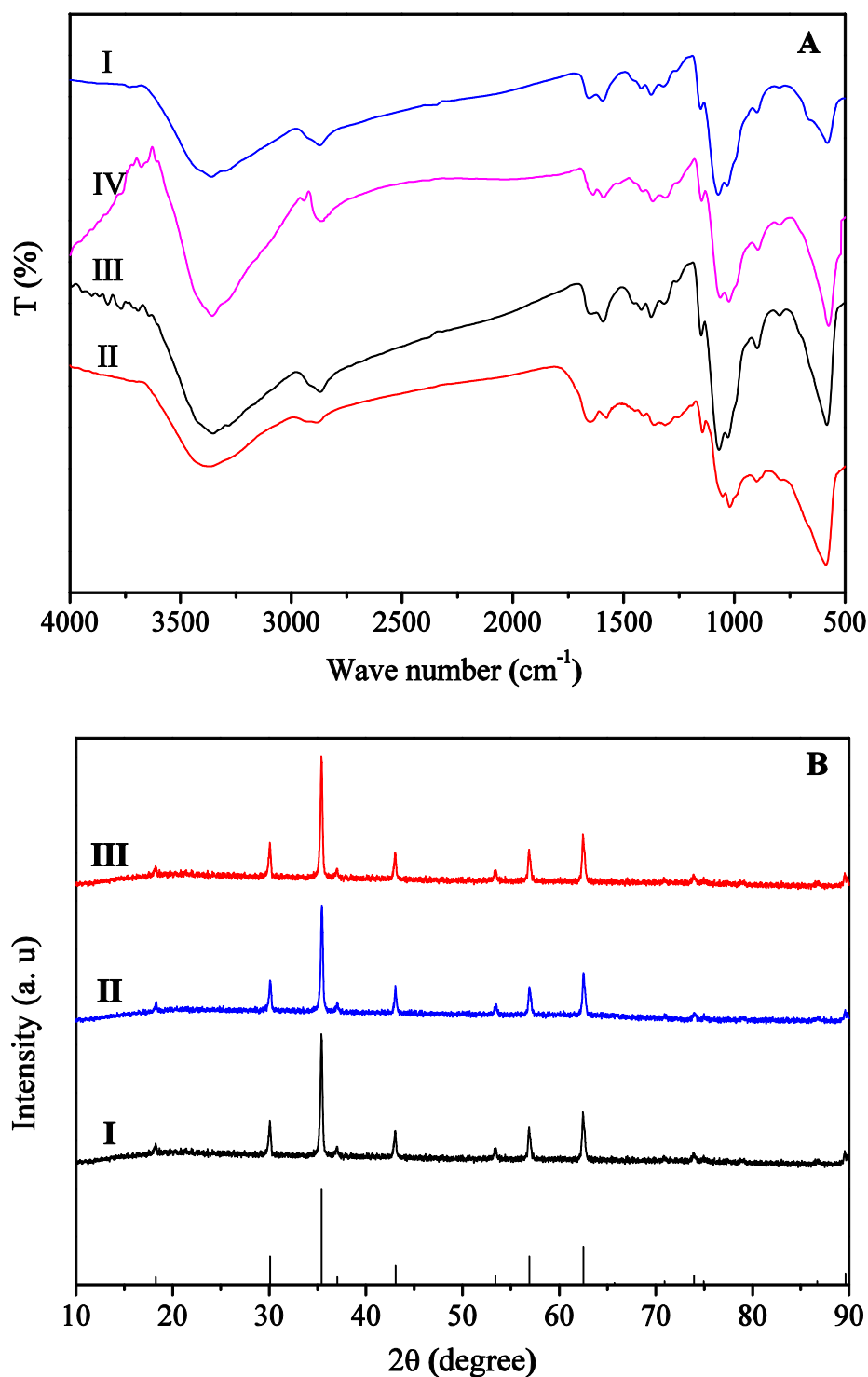


Fig. S4 (A) FTIR spectra of MCBs stored at different magnetic fields original MCBs(I), 0.2 T(II), 0.3 T(III) and 0.4 T (IV). (B) XRD of MCBs stored at different magnetic fields (0.2 T(I), 0.3T (II) and 0.4 T(III)). (Literature values for the peak positions and intensities for bulk magnetite samples are indicated by the vertical bars).

Supplementary Material references

- S1. D. Singh, Adsorpt Sci Technol, 2000,18, 741-748.
- S2. J.W. Biggar, M.W. Cheung, Soil Sci. Soc. Am., Proc, 1973, 37, 863-868.
- S3. Y.H. Li, Z. Di, J. Ding, D. Wu, Z. Luan, Y. Zhu, Water Res, 39 (2005) 605–609.